



Selecting Double-Base Propellants for a 120 mm Mortar Rocket Assisted Projectile through DoE

L. A. I. Pires, V. V. V. da Silva, F. C. Peixoto and E. P. de Araújo*

Military Institute of Engineering, Rio de Janeiro, RJ, Brazil

The manuscript was received on 9 February 2025 and was accepted after revision for publication as an original research paper on 30 May 2025.

Abstract:

Range extension of a 120 mm mortar projectile can be attained by a rocket motor within the grenade body. This study deals with the design of experiments-based methodology to identify double-base propellant compositions conceptually feasible for such a motor, from a thermochemical viewpoint. Formulations were defined under low vulnerability and green principles, using Minitab® Statistical Software, following mixture design techniques to account for intrinsic constraints. The thermochemical behavior of these formulations was simulated with a specialized software, taking theoretical characteristic velocity c^ as a performance indicator. An empirical model was then fitted, permitting the identification of a set of favorable compositions leading to c^* enhancement, regarding a reference double-base propellant, thus unveiling the design possibility of rocket motor downsizing.*

Keywords:

rocket assisted projectile, design of experiments, characteristic velocity, low vulnerability ammunition, green propellants

1 Introduction

Range extension and the accuracy of artillery shells are paramount in modern warfare [1]. Extending the range allows for striking targets deep within enemy territory, while also enabling howitzers and mortars to be positioned in safer tactical locations within friendly zones [2]. Providing additional thrust to the flying artillery shell by means of an embedded solid propellant rocket motor, properly ignited after the grenade is expelled from the bore, is a well-known way to achieve range extension [2-4]. This solution, known as rocket-assisted projectile (RAP), presents the penalty of reducing the free internal volume available in the shell for the explosive filling, but imparts the

* Corresponding author: Military Institute of Engineering, Praça Gen Tiburcio, 80, Urca, Rio de Janeiro, RJ, Brazil, BR-22290-270. Phone: +55 21 25 46 71 21, E-mail: emmanuel-paraujo@ime.eb.br. ORCID: 0000-0003-3269-9664.

projectile with higher range extensions as compared to base bleed units [5]. On the other hand, it shares the constraint of hindering the ammunition precision and accuracy levels with the latter [2, 5], while its effectiveness also depends on factors such as firing angle [5-7], atmospheric conditions [8], mass ratio between the solid propellant and the round [5, 9], aerodynamic form of the projectile [6] and rocket motor ignition delay [4-6].

Mortar systems with a caliber of 120 mm seem particularly suitable for the application of rocket assisted projectiles, for they are known to suffer from limited range as compared to heavier artillery systems, but offer, on the other hand, a desirable combination of advantages in the field, i.e., high mobility, good rate of fire, low maintenance requirements, fast readiness into action and the possibility to be concealed [2]. Compared to 105 mm and 155 mm artillery systems, 120 mm mortars can provide higher lethality and better logistics, respectively [10]. The insertion of a rocket motor within the 120 mm projectile seems an effective way to extend its range without hampering the mortar's mobility [2].

Double-base solid propellants consisting of a homogeneous structure comprising a nitrocellulose matrix plasticized by nitroglycerine, along with tailoring additives [3, 11], have been applied to 120 mm mortar shell assisted propulsion [12]. In spite of their lower specific impulse as compared to typical composite solid propellants [13], they are not usually jeopardized by smoky and corrosive exhaust, moisture sensitivity and two-phase performance loss issues of the latter [3, 14, 15]. A range increase of up to 20 %, referred to an inert shell, has been reported for a double-base propellant [4]. When applied to rocket motors, such propellants are required to exhibit specific mechanical qualities, so far mostly attained with the aid of phthalate plasticizers, for instance, dibutyl and diethyl phthalate [3, 11, 16]. As for their burn rates, they are commonly expected to yield super rate and plateau/mesa behaviors [11, 15], which allow the rapid attainment of the nominal chamber pressure and the relative stability of burn rate within a certain pressure domain, respectively [3, 13]. Apart from performance considerations, the suitability of solid propellants to rocket applications has been increasingly constrained by low vulnerability and environmental friendliness requirements [3, 17, 18].

Low vulnerability of ammunition to unplanned stimuli has been a paramount engineering topic in the last decades [19]. The existence of notably active research [20] and industrial [21] forums dealing with the topic features the importance of matching performance and risk mitigation in the modern warfare. In this sense, 120 mm mortar conventional [22] and rifled [12] systems have been revamped to adhere to low vulnerability criteria, with a focus on the explosive filling replacement, on the warhead venting and on packaging improvements. From the rocket motor viewpoint, the incorporation of the crystalline nitramines cyclotrimethylene trinitramine (RDX) and cyclotetramethylene tetranitramine (HMX) to double-base propellant formulations may contribute to reduce sensitivity [23-25], while favoring chemical stability [26, 27] and smoke and signature reduction [3]. Impact and friction sensitivity of double-base propellants containing both micro and nano-RDX particles were assessed, suggesting the important role of particle size in mitigating these sources of inadvertent ignition [28, 29]. RDX or HMX-added double-base propellants can be labelled as part of the composite-modified double-base propellants (CMDDB) family [3, 14].

As for environmental friendliness, the impacts stemming from the entire lifecycle of energetic materials have received ever increasing attention [30, 31]. Regarding double-base propellants, this constraint should be reflected in the qualitative and quan-

titative selection of propellant formulations, taking into account available data on the risks posed by chemical substances [32], particularly lead-based burn rate modifiers and phthalate plasticizers, for their remarkable harmful effect on human health and on the environment [33]. The former are required to provide super-rate, plateau and/or mesa behaviors according to Vielle's law and depending on the specific rocket motor mission profile [3, 11, 34], but are quite toxic chemicals [33]. Apparently, an ideal burn rate catalyst that can substitute lead-based chemicals while simultaneously ensuring appropriate ballistic performance and environmental adequacy has not yet been identified [35], despite some promising bismuth-based compounds [35-37]. By their turn, dibutyl phthalate is suspected of damaging fertility and is quite toxic to aquatic life, while diethyl phthalate is currently under investigation as an endocrine disrupting agent [33]. Some alternatives in the citrates family have been successfully investigated [37, 38]. For instance, acetyl tributyl citrate (ATBC) is a widespread phthalate substitute plasticizer, so far recognized as an ecofriendly chemical, and has been largely used in products such as food packaging, vinyl toys and pharmaceutical excipients [39]. Yielding melting and boiling points of $-80\text{ }^{\circ}\text{C}$ and $331\text{ }^{\circ}\text{C}$, respectively [39], ATBC has been reported as part of a double-base propellant formulation [40].

The preliminary selection of solid propellant formulations to address performance, sensitivity and environmental constraints may be rationalized if a performance-related figure of merit is used. In this sense, characteristic velocity, usually denoted by c^* , seems a suitable parameter, for it reflects solely the thermochemical performance of the propellant in the combustion chamber, while keeping a directly proportional relation to rocket motor thrust, specific impulse and vehicle velocity increase in drag-free vacuum [3, 41]. Consequently, range extension in rocket-assisted artillery would benefit from c^* maximization. Theoretical characteristic velocity is a preliminary design parameter for rocket motors [3, 9, 42], ranging from circa 1 200 m/s to roughly 1 700 m/s in low and high-performance solid propellants, respectively [3, 9]. Specialized computer codes such as NASA Chemical Equilibrium with Applications (NASA CEA) [43, 44] are frequently used to estimate it [3, 42].

In this context, the mass ratios of solid propellant components for c^* calculations can be derived from mixture modelling, a Design of Experiments (DoE) tool. It addresses problems in which a response variable depends on the component's proportions of a mixture [45, 46]. The fitting of Scheffé-type mixture models to experimental data may clarify the role played by each component in the response variable and shed light on their relevant interactions, thereby leading to the identification of favorable formulation regions and sequential improvement paths, depending on the objectives of the experimenter [45, 46]. Hybrid propulsion studies have been conducted under mixture modelling guidelines [47, 48]. In addition, statistical software can be useful in building experimental matrices, model fitting and interpretation [49]. Moreover, applying DoE techniques to computer-generated data, particularly those stemming from deterministic models leading to unreplicated responses [50], such as theoretical c^* , provides the basis for the rational screening of suitable solid propellant formulations, given their ingredients have been chosen under sensitivity attenuation and environmental friendliness criteria. An unreplicated mixture design has been applied to a chemometric investigation allowing coherent chemical interpretations [51].

Therefore, this paper deals with a methodology based on mixture modeling to preliminarily select, from a thermochemical point of view, feasible candidate double-base solid propellant formulations for the rocket-assisted propulsion of a 120 mm mortar projectile. The candidate formulations adhere to low vulnerability and green

principles, and their calculated performances are expected to positively impact design trade-offs among shell range extension, accuracy, and terminal effects. This overall approach intends to rationalize costly, time-consuming trial-and-error experimental schemes.

2 Experimental Section

2.1 Qualitative and Quantitative Definition of Formulations of Propellants

The methodology herein discussed requires a reference double-base propellant formulation, conceptually applicable to the motor of a 120 mm rocket-assisted projectile. Such formulation should yield super rate burning behavior, given the usual short rocket motor functioning period of roughly 3.0 to 7.0 s [6, 7, 52], thus imposing the quick attainment of the plateau regime. This can be effectively done by means of lead and copper-based compounds, whose performance seem to outweigh their environmental risks, even considering ecofriendly alternatives so far assessed [35, 37]. Hence, this work takes the lead-based formulation presented in Tab. 1 as a reference, which is adapted from data displayed by Kubota [15, 34] for a double-base propellant capable of providing both super rate and plateau burning. Nitrocellulose with a 12.6% nitrogen content was chosen due to its applicability to rocket propellant formulations [11]. Graphite was included, given its role in enhancing super-rate burning [15, 34]. Chemical species are accompanied by acronyms, to identify them in subsequent presentation and discussions of the results.

The modified double-base propellant formulation was qualitatively defined under sensitivity and green perspectives, keeping in mind its performance. Thus, starting from the reference formulation, RDX, which is expected to act as a less-sensitive energetic component, was incorporated in an amount comparable to some studies on the inclusion of nitramines into double-base propellants [14, 27, 53, 54], at the expense of the combined amounts of nitrocellulose and nitroglycerine. Besides, lead 2-ethylhexoate and diethyl phthalate were replaced by copper salicylate and acetyl tributyl citrate (ATBC), respectively. The first substitution stems from the data suggesting a synergistic effect between lead and copper salicylates in enhancing super rate burning [15, 34]. As an additional benefit, this replacement reduces the total lead amount in the investigated formulations. In the 120 mm mortar context, ATBC should provide the mechanical qualities required by the rocket assisted projectile mission without environmental harmful effects.

The modified double-base propellant formulation, hereinafter stated as a composite modified double-base formulation (CMDB), is depicted in Tab. 1. It should be noted that the total amounts of inert plasticizer, ballistic modifiers and graphite are the same as in the reference formulation. Tab. 1 presents the main function, as well as lower and upper mass ratio (wt%) limits for each CMDB ingredient. These limits are inputs for defining the experimental domain and were set taking CMDB nominal mass ratios as middle points. Their magnitudes are intended to allow proper variability for each component, thus avoiding the construction of an over restrained experimental region [45]. The simultaneous inclusion of lead, copper and graphite in this CMDB formulation is also related to literature data showing that the most effective ballistic modifier in double-base propellants is provided by lead compounds alongside with copper oxide and solid carbon particles [35]. Moreover, a nitramine (HMX) has been

reported to yield super-rate and plateau burning rate profile in a CMDB formulation containing a lead compound [15].

In Tab. 1, particular attention should be paid to RDX, plasticizers and burn rate modifiers, for they comprise the qualitative changes from reference to CMDB formulations. In short, by reducing nitroglycerine and lead-based ballistic modifier amounts and replacing the phthalate plasticizer, the CMDB formulation, although not ideal, provides a potentially less harmful picture under green and low vulnerability constraints.

Tab. 1 Reference and CMDB propellant formulations

Item	Reference formulation	CMDB formulation			Main function [3]
	Nominal mass ratio [wt%]	Lower mass ratio limit [wt%]	Nominal mass ratio [wt%]	Upper mass ratio limit [wt%]	
Nitrocellulose 12.6%N (NC)	51.0	39.0	44.0	49.0	Energetic matrix
Nitroglycerine (NGL)	37.0	27.0	32.0	37.0	Energetic plasticizer
Ethyl centralite (EC)	1.8	1.3	1.8	2.3	Stabilizer
RDX	-	7.0	12.0	17.0	Energetic filler
Diethyl phthalate (DEP)	7.0	-	-	-	Inert plasticizer
Acetyl tributyl citrate (ATBC)	-	4.0	7.0	10.0	Inert plasticizer
Lead salicylate (PbSalic)	1.5	0.5	1.5	2.5	Burn rate modifier
Lead 2-ethylhexoate (PbEtHex)	1.5	-	-	-	Burn rate modifier
Copper salicylate (CuSalic)	-	0.5	1.5	2.5	Burn rate modifier
Graphite	0.2	0.1	0.2	0.3	Opacifier/super rate burning

2.2 Construction of the Experimental Domain Through Mixture Modelling

Minitab[®] Statistical Software, version 22, was applied to build the original experimental matrix for CMDB formulations, from the mass ratio ranges depicted in Tab. 1. Such matrix contains all the possible propellant formulations given its number of components. As CMDB formulations comprise eight components with non-uniform mass ratio ranges, the corresponding extreme vertices design leads to a hyperpolyhedral experimental domain [45]. Besides, current industrial practice in the production of solventless extruded double-base propellants starts with a paste, comprising at least nitrocellulose, nitroglycerine and a stabilizer, to which other raw materials are subsequently added to define the propellant formulation [11]. Therefore, linear restrictions

[45] were imposed on the three constituents of the paste, to assure that their mass ratios remain nearly constant throughout the experimental matrix, provided they are not further added after propellant paste production. Considering the data on Tab. 1, these linear restrictions, as applied to CMDDB formulations, are expressed in Tab. 2.

Tab. 2 Linear restrictions stemming from propellant paste formulation

Propellant paste constituents	Mass ratios codification (wt%)	Linear restrictions on mass ratios
Nitrocellulose 12.6%N	A	
Nitroglycerine	B	$0.72 \leq B/A \leq 0.74$
Ethyl centralite	C	$0.040 \leq C/A \leq 0.042$

A Scheffé type special cubic model for the CMDDB formulation with eight components comprises 92 terms [45]. Given the deterministic nature of the response variable and the absence of replicates for c^* in this work, estimating the lack of fit error required an excess of experimental points. Therefore, an initial set of 9 excess points was defined for the CMDDB formulations, resulting in a total of 101 double-base propellant formulations selected from the original experimental matrix generated by Minitab®. The selection was based on distance optimality criterium, so that the design points are located in an evenly manner throughout the experimental region. Such a distribution is particularly suitable for deterministic responses [50].

The model fitted to the theoretical characteristic velocities comprised single, two and three-component effects, which seems reasonable for initial screening purposes [45]. Next, the model was simplified through the elimination of non-significative terms, by applying the backward elimination built-in Minitab® tool. The resulting reduced Scheffé polynomial had its quality checked through graphical analysis of the residuals [51].

2.3 Thermochemical Calculations

Theoretical characteristic velocity was computed for each double-base propellant formulation defined under the aforementioned criteria through NASA CEA “rocket problem” routine [43, 44]. The following settings were adopted: adiabatic combustion and isentropic expansion, shifting equilibrium performance, chamber pressure of 6.89 MPa (68.9 bar), optimum expansion to ambient pressure at sea level (1.01325 bar), initial chamber temperature of 3 800 K and combustion chamber cross section/throat area ratio of 9.0. The last setting is related to the attainment of stagnation conditions in the chamber [3]. NASA CEA requires molecular formulas and standard enthalpies of formation (ΔH_f°) for each propellant’s component. These are inputs for computing the reaction’s enthalpy once the equilibrium composition of the gas has been determined through Gibbs free energy minimization [41, 43, 44].

Input data are listed in Tab. 3. Standard enthalpies of formation for lead and copper salicylates were not identified in reference literature [25, 55-58]. As a consequence, they were estimated according to the method suggested by Vatani et al. [59].

Tab. 3 Standard enthalpies of formation for the selected propellant ingredients

Item	Molecular formula	ΔH_f° (kJ/mol)	Reference
Nitrocellulose 12.6%N	$C_{12}H_{15.10}O_{19.80}N_{4.90}$	-1414.71	[25]
Nitroglycerine	$C_3H_5N_3O_9$	-370.72	[25]
Ethyl centralite	$C_{17}H_{20}N_2O$	-105.08	[25]
RDX	$C_3H_6N_6O_6$	66.94	[25]
Diethyl phthalate	$C_{12}H_{14}O_4$	-753.08	[55]
Acetyl tributyl citrate	$C_{20}H_{34}O_8$	-1848.00	[55]
Lead salicylate	$C_{14}H_{10}O_6Pb$	-1313.29	[59]
Lead 2-ethylhexoate	$C_{16}H_{30}O_4Pb$	-1494.13	[25, 59]
Copper salicylate	$C_{14}H_{10}O_6Cu$	-1313.29	[59]
Graphite	C	0.00	[55]

2.4 Effect of Selected Propellant Formulations on the Design of a 120 mm Rocket Assisted Mortar Shell

Experimental results and computer simulations suggest that the required average thrust for a 50% maximum range extension of a 120 mm mortar shell can be approximately taken as 850 N [7]. This maximum range increment is referred to an identical 120 mm mortar shell, except for the rocket assisted propulsion unit, launched under the same elevation degree and similar muzzle velocities [7]. The 850 N thrust level seems coherent with literature data on RAP [4]. Subsequently, by selecting a theoretical c^* and its NASA CEA calculated thrust coefficient (C_F), as well as by defining the required thrust (F), propellant mass flow rate (\dot{m}) was estimated through the ideal rocket equation [3]:

$$\dot{m} = \frac{F}{C_F c^*} \quad (1)$$

Eq. (1) determined the \dot{m} threshold from which the selected double-base propellant formulations would meet the thrust requirement for a 120 mm mortar grenade 50 % maximum range increment [7]. By its turn, knowledge of \dot{m} threshold for a given estimated range extension may lead to trade-off considerations between the rocket motor sizing, the explosive filling weight, and the accuracy of the round. Such an analysis seems appropriate given the inherently low accuracy of dumb rocket assisted mortar shells [2], which conceptually could be compensated, in terms of terminal effects, by a larger amount of explosive filling, or conversely, have their accuracy improved by trajectory correction devices.

3 Results and Discussions

3.1 Experimental Matrix, Thermochemical Results, Model Fitting and Interpretation

Theoretical characteristic velocity for the reference formulation described in Tab. 1 amounted to 1 405.10 m/s. Accordingly, its calculated thrust coefficient and specific

impulse at nozzle exit, under optimum expansion to sea level atmospheric pressure, reached 1.5731 and 225 s, respectively.

The software-aided definition of an extreme vertices' mixture design for the CMDB formulation depicted in Tab. 1 required mass ratio limits for each of its eight components, the linear restrictions previously discussed and expressed in Tab. 2, as well as the degree of the model to be fitted. Given the preliminary screening nature of this study, a third-degree model was selected. These settings led to the construction of a hyperpolyhedric experimental region comprising a total of 1 885 points, each of them yielding a different CMDB propellant formulation. The nature of these design points and their distribution according to their dimension is presented in Tab. 4. For instance, point type "0" with dimension "7" is the centroid of the hyperpolyhedrum. No replicates were included, due to the deterministic character of theoretical c^* [50]. It should be noticed that the chosen degree of the model restricts the point types used in the construction of the experimental region. As a result, there are no points of dimension 3, 4, 5 and 6, as shown in Tab. 4.

Tab. 4 Number of design points for each type

Point Type	1	2	3	4	5	6	7	0	-1
Dimension	0	1	2	3	4	5	6	7	0
Distinct	176	616	916	0	0	0	0	1	176
Replicates	1	1	1	0	0	0	0	1	1
Total number	176	616	916	0	0	0	0	1	176

Subsequently, the criterium of distance optimality was applied to select 101 experimental points out of the 1 885 initially available. For each of the selected CMDB propellant formulations, theoretical c^* was estimated through NASA CEA under the previously described settings, with run order randomized by Minitab® software. Formulations and their theoretical c^* results for a sample of 11 out of the 101 points in the extreme vertices mixture design subset are presented in Tab. 5, in decreasing order of characteristic velocity. This sample comprises the 5 highest and 5 lowest c^* results. Point type "0" is highlighted in bold.

Theoretical c^* ranged from 1336.5 m/s to 1487.7 m/s, with a mean value of 1 414.76 m/s and a standard deviation of 37.92 m/s. The centroid formulation yielded a theoretical c^* close to the mean value. At the 5% level of significance, Dixon's Q test showed that there were no outliers. The decisions made when setting up the initial experimental region, for instance the degree of the model, the range of components' mass ratios and the selection of formulation points through distance optimality criterium, have obviously restricted the variability of formulations and consequently that of theoretical c^* . The choice of the model degree, although coherent with the screening purposes of this study, prevented a thorough representation of the multidimensional experimental domain. This can be confirmed by noticing, in Tab. 4, that there were no formulations corresponding to 3, 4, 5 and 6 dimensions, which would allow, respectively, the fitting of 4th, 5th, 6th and 7th degree interaction terms.

Theoretical c^* model fitting was conducted through Minitab® built-in backward elimination technique, which consists in successively fitting special cubic Scheffé-type models, beginning with the complete set of 92 terms, and then eliminating the ones with a p-value greater than a limiting threshold (in this study, 0.050) and refitting the model. This iterative process led to the special cubic model with 66 terms detailed in Tab. 6. Standard errors and p-values for each estimated coefficient are also presented.

Tab. 5 Formulations and c^ sample results – extreme vertices mixture design as applied to CMDB formulations*

Point Type	NC [wt%]	NGL [wt%]	EC [wt%]	RDX [wt%]	ATBC [wt%]	PbSalic [wt%]	CuSalic [wt%]	Graphite [wt%]	NASA CEA c^* [m/s]	Fitted c^* [m/s]	Residuals [m/s]
1	0.4420	0.3183	0.0177	0.1700	0.0400	0.0050	0.0050	0.0020	1487.70	1487.65	0.05
2	0.4635	0.3430	0.0185	0.1229	0.0400	0.0050	0.0050	0.0020	1483.30	1483.35	-0.05
3	0.4339	0.3167	0.0174	0.1700	0.0400	0.0150	0.0050	0.0020	1477.60	1477.58	0.02
1	0.4900	0.3626	0.0196	0.0758	0.0400	0.0050	0.0050	0.0020	1476.80	1476.78	0.02
1	0.4900	0.3528	0.0196	0.0856	0.0400	0.0050	0.0050	0.0020	1475.90	1475.92	-0.02
0	0.4394	0.3207	0.0180	0.1198	0.0698	0.0148	0.0148	0.0025	1417.70	1417.56	0.14
1	0.3900	0.2808	0.0156	0.1606	0.1000	0.0250	0.0250	0.0030	1349.40	1349.34	0.06
1	0.3900	0.2886	0.0164	0.1520	0.1000	0.0250	0.0250	0.0030	1349.10	1349.10	0.00
3	0.4441	0.3242	0.0187	0.0700	0.1000	0.0150	0.0250	0.0030	1349.00	1348.93	0.07
2	0.4130	0.3056	0.0173	0.1110	0.1000	0.0250	0.0250	0.0030	1342.80	1342.71	0.09
1	0.4360	0.3227	0.0183	0.0700	0.1000	0.0250	0.0250	0.0030	1336.50	1336.51	-0.01

The fitted model comprises linear, quadratic, and special cubic terms. It should be noticed that among linear terms, the one corresponding to RDX mass ratio is the sole positive, which is coherent with the expected effect of its positive standard enthalpy of formation in enhancing the reaction's heat. In addition, binary and ternary contributions significantly affect theoretical c^* as well, both synergistically (positive signal) and antagonistically (negative signal). All the binary interaction terms bear a positive sign, thus increasing theoretical c^* , while among the 38 ternary interaction terms, only 14 bear a positive sign, and thus synergistically contribute to characteristic velocity. It is not advisable, however, to draw conclusions solely from the individual or grouped interpretation of coefficients' magnitudes and signals [45, 51].

Dealing with pseudo-experimental results, for which replication is of no use, residuals analysis can provide information on model quality [45, 51]. Minitab® analysis of fitted c^* and their corresponding residuals are depicted in Fig. 1, in which the residuals/fitted value (c) and residuals/observation order (d) plots do not suggest systematic tendencies. At the same time, the histogram of the residuals (b) shows a quasi-normal distribution, while normal probability plot (a) confirms this interpretation. Hence, the special cubic Scheffé-type model herein fitted to theoretical c^* (c^* -star) data seems suitable for the preliminary screening purpose of this work, despite its intentionally limited representation of the seven-dimensional experimental domain.

The individual effects of components on fitted c^* can be clarified by means of a Cox response trace plot depicted in Fig. 2. It is a plot of c^* , obtained from the fitted model, along Cox' directions. These are particular paths within the experimental region which allow measuring the effect of a component while keeping the ratios among the other components identical to the ones existing in a reference blend [45]. This mixture modelling tool seems particularly useful for the interpretation of models comprising a large number of terms, such as the one detailed in Tab. 6.

The reference blend, labelled in Fig. 2 as "Comp:RefBlend", is usually selected as the centroid formulation [45] highlighted in Tab. 5, which attained a 1417.70 m/s theoretical c^* . One can notice, by examining Tab. 5 and Fig. 2, that the reference blend does not lead to c^* maximization within the experimental range. The idea here is to estimate the effects of small deviations, both positive and negative, on the fitted c^* , for each component from the centroid, for it frequently yields the average behavior in the experimental domain [45], thereby providing a convenient reference blend.

Tab. 6 Estimated Regression Coefficients for c^* [m/s] (component proportions)

Term	Coefficient	SE Coefficient	P-Value
NC	-34069	6766	*
NGL	-3799	2080	*
EC	-7865815	1701446	*
RDX	300	612	*
ATBC	-8314	1584	*
PbSalic	-5719	1551	*
CuSalic	-21346	3640	*
Graphite	-350421	69149	*
NC*NGL	75818	13598	0.000
NC*EC	8598136	1871470	0.000
NC*RDX	39139	7984	0.000
NC*ATBC	92569	14431	0.000
NC*PbSalic	353424	72298	0.000
NC*CuSalic	375980	72652	0.000
NC*Graphite	5998020	1033456	0.000
NGL*EC	6197799	1440527	0.000
NGL*ATBC	31335	8986	0.001
NGL*CuSalic	76327	10565	0.000
NGL*Graphite	10323357	1787510	0.000
EC*RDX	8081406	1736948	0.000
EC*ATBC	6600107	1803959	0.001
EC*Graphite	42064676	10924186	0.000
RDX*ATBC	10646	3418	0.004
RDX*CuSalic	25442	4859	0.000
ATBC*PbSalic	65087	10178	0.000
ATBC*Graphite	1715559	315175	0.000
PbSalic*Graphite	5006672	949677	0.000
CuSalic*Graphite	4430568	855524	0.000
NC*NGL*EC	2834557	624707	0.000
NC*NGL*ATBC	-68495	37600	0.000
NC*NGL*PbSalic	-778791	166139	0.000
NC*NGL*CuSalic	-830075	165411	0.000
NC*NGL*Graphite	-30832150	5307982	0.000
NC*EC*ATBC	686584	290821	0.024
NC*EC*Graphite	-68711666	20355389	0.002
NC*RDX*PbSalic	-213784	51514	0.000
NC*RDX*CuSalic	-230708	50234	0.000
NC*RDX*Graphite	-6832771	1271288	0.000
NC*ATBC*PbSalic	-605656	100759	0.000
NC*ATBC*CuSalic	-684333	99050	0.000
NC*ATBC*Graphite	-4960475	1341206	0.001
NC*PbSalic*CuSalic	-1103275	309002	0.001
NGL*EC*RDX	1275080	306298	0.000
NGL*EC*ATBC	4294115	972854	0.000
NGL*EC*PbSalic	21787162	4583966	0.000
NGL*EC*CuSalic	19916483	4417537	0.000
NGL*RDX*ATBC	-24381	10454	0.026
NGL*RDX*PbSalic	91042	24474	0.001
NGL*RDX*Graphite	-9807910	1780174	0.000
NGL*ATBC*PbSalic	-103835	49807	0.044
NGL*ATBC*Graphite	-11699330	2009373	0.000
NGL*PbSalic*Graphite	-22268005	4496908	0.000
NGL*CuSalic*Graphite	-29299007	4934760	0.000
EC*RDX*PbSalic	3870698	1807987	0.001
EC*RDX*CuSalic	4118502	1118698	0.001
EC*ATBC*PbSalic	15147019	2323830	0.000
EC*ATBC*CuSalic	18270556	2664644	0.000
EC*ATBC*Graphite	-84218097	18351428	0.000
EC*PbSalic*CuSalic	29092702	8242259	0.001
EC*PbSalic*Graphite	-154492825	30519924	0.000
RDX*ATBC*PbSalic	-54166	10962	0.000
RDX*ATBC*CuSalic	37758	6881	0.000
ATBC*PbSalic*CuSalic	70631	26999	0.013
ATBC*PbSalic*Graphite	-13223819	2101893	0.000
ATBC*CuSalic*Graphite	-13329539	2092325	0.000
PbSalic*CuSalic*Graphite	-17478578	5688769	0.004

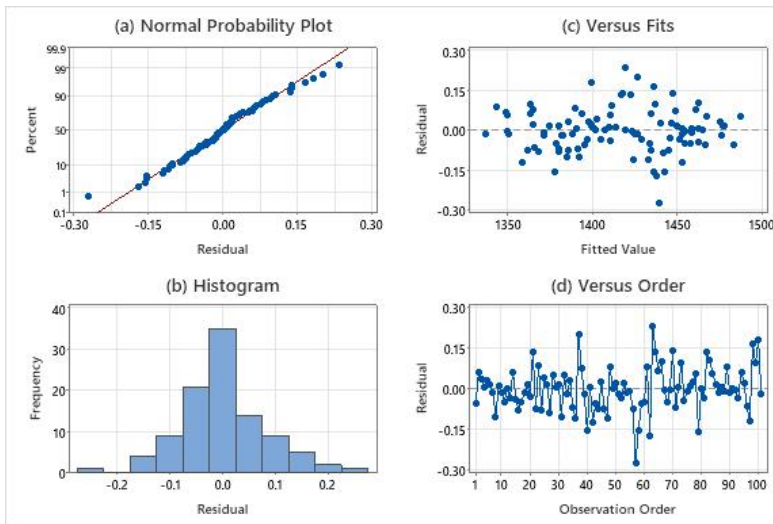


Fig. 1 Residuals plots of theoretical c^*

This approach provides a more direct assessment of the role of individual components in the response variable as compared to the interpretation of the model's coefficients.

Fig. 2 shows that nitroglycerine and RDX have a constant theoretical c^* increasing tendency within the deviation range considered. On the other hand, nitrocellulose and ethyl centralite exhibit a maximum-like behavior near the reference blend, while ATBC shows a consistently decreasing trend in the fitted c^* values. Augmenting both ballistic modifiers amounts results in a decreasing c^* fashion, while graphite plays, as expected, a negligible role. Moreover, Cox response trace plot showed a remarkable effect of nitrocellulose on the fitted c^* , which is expected from its major proportion in the formulations herein investigated. In addition, RDX and ATBC also imparted significant effects on c^* , with clearly opposite results under either positive or negative deviations from the reference blend. The burn rate lowering tendency as a result of RDX addition into double-base rocket propellant formulations, regardless of the associated specific impulse enhancement, has been pointed out [54]. On its turn, definition of ATBC mass ratio should stem not only from thermochemical considerations, but also from its effect on mechanical performance of the propellant, a relevant aspect under the expressive accelerations to which a rocket assisted projectile is subjected [2, 3].

Pb and Cu-based ballistic modifiers also showed themselves capable of penalizing theoretical c^* . Besides, their proportions affect super-rate and plateau burning regimes, and as a consequence, overall rocket motor performance [3, 15]. To identify suitable candidate formulations for double-base propellants from a thermochemical perspective, it is advisable to select independent composition variables based on raw materials that enhance low vulnerability and environmental friendliness. These formulations can then be experimentally assessed under multiple performance criteria. Thus, the fitted model can be simplified through the choice of convenient values for nitrocellulose and graphite and by examining the three-dimensional experimental regions comprising each of the ballistic modifiers, as well as RDX and ATBC.

This approach was carried out by generating two contour plots in Minitab®, from the fitted c^* model presented in Tab. 6. The first one comprises RDX, ATBC and PbSalic mass ratios, while the second one has RDX, ATBC and CuSalic mass ratios to variate. The resulting contour plots are depicted in Figs 3a and 3b, respectively. The enhanced trapezoidal constraint regions in both contour plots stem from the upper and lower mass ratio limits adopted for the components and described in Tab. 1. Additionally, Figs 3a and 3b state, under the “Hold Values” label, the constant proportions defined for the components not included in the ternary diagrams, which are those from the reference blend in Fig. 2. In both contour plots, the increasing c^* pattern towards larger RDX proportions is dominant.

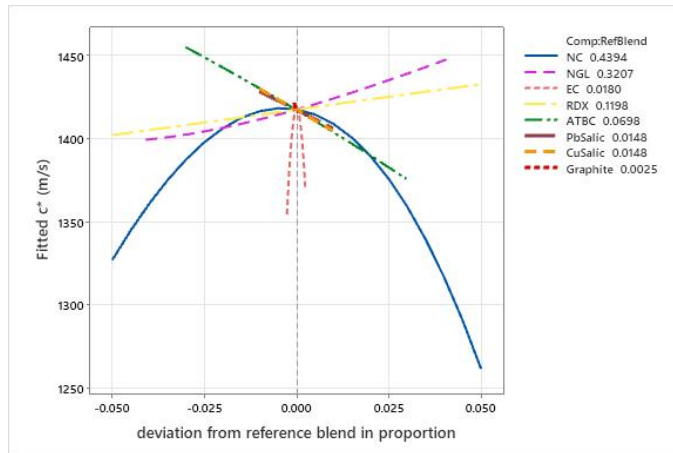


Fig. 2 Cox response trace plot of fitted c^* – centroid as the reference blend

From each of the trapezoidal constraint regions, two conceptually feasible double-base propellant formulations are sorted with their respective theoretical c^* predictions, according to the fitted Scheffé polynomial. These compositions are intended to illustrate the possibilities brought by the methodology discussed in this work. Accordingly, these high-performance formulations from each ternary diagram are organized in Tab. 7 alongside with their c^* predictions, identified as “A” and “B” in Fig. 3a and as “C” and “D” in Fig. 3b. The Maximum c^* value attained within the experimental region is also depicted in Tab. 7.

Running NASA CEA c^* calculation for A, B, C, and D formulations allows a check on model quality under a confirmatory experiment procedure [45]. Relative deviations quantify the adherence of predicted c^* to NASA CEA c^* . Calculated thrust coefficient (C_F) and specific impulse at nozzle exit, under optimum expansion to sea level atmospheric pressure (I_{sp}), are also presented.

The attained relative deviations were quite acceptable, particularly for the maximum c^* formulation. As previously concluded from residual analysis, the confirmatory experiments presented in Tab. 7 suggest the fitted Scheffé polynomial acceptable capacity to predict theoretical c^* results, in a preliminary screening study, particularly in the vicinities of the formulations associated to model fitting. Nevertheless, it is necessary to consider its intrinsic prediction limitations, particularly when selecting a CMDB formulation as a starting point for an optimization path. This implies that relative deviations are likely to increase for CMDB compositions that deviate from the experimental points used to fit the Scheffé polynomial.

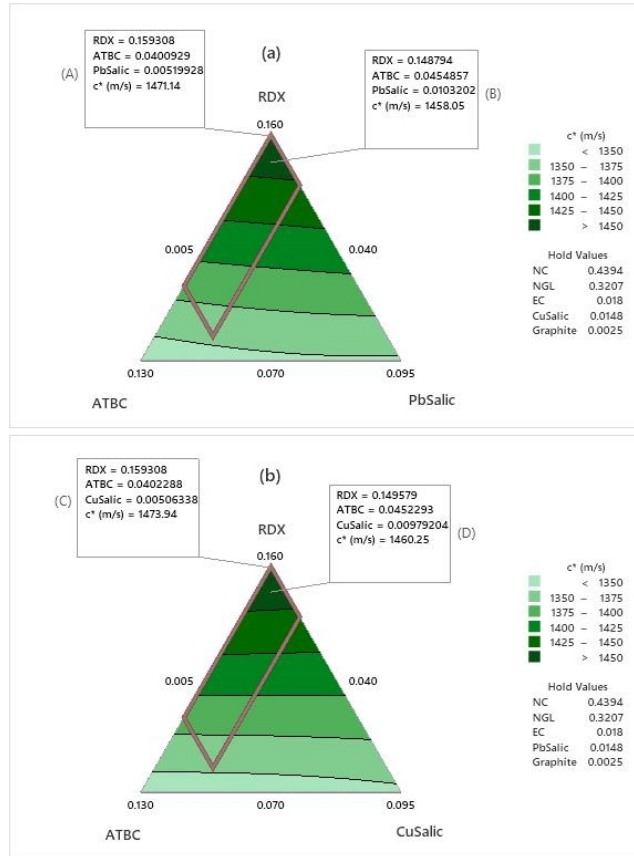


Fig. 3 Contour plots for theoretical c^* – RDX-ATBC-PbSalic (a) and RDX-ATBC-CuSalic (b)

As for the Maximum c^* CMDB formulation, its characteristic velocity enhancement, as compared to A, B, C and D compositions, results from the simultaneous reduction of lead and copper-based ballistic modifiers to their lower mass ratios and the setting of RDX to its upper mass ratio limit, given the proximity among the remaining components' mass ratios to A, B, C and D formulations. Maximum c^* formulation, although ideal from the thermochemical viewpoint and potentially desirable from environmental and low vulnerability perspectives, may not meet ballistic performance criteria, specifically super-rate, and plateau regime at an acceptable burning rate level, given its intended application in a 120 mm rocket assisted projectile. In this scenario, the experimental assessment of burn rates within a defined pressure range seems mandatory to bring a paramount response variable into consideration.

Bearing in mind that NASA CEA c^* for the reference double-base propellant described in Tab. 1 was 1405.10 m/s, the corresponding characteristic velocity relative increments provided by CMDB formulations in Tab. 7 were 4.80 % (A), 3.80 % (B), 4.94 % (C), 3.96 % (D), and 5.88 % (Maximum). These increments, although modest, may represent an initial step towards trade-off efforts aimed at balancing the volumes occupied by explosive filling and by the rocket motor in a volume-restricted system such as a 120 mm mortar shell.

Tab. 7 Initially selected candidate CMDB propellant formulations

Propellant components	RDX/ATBC/PbSalic formula- tions (wt%)		RDX/ATBC/CuSalic formula- tions (wt%)		Maximum c^* formulation (wt%)
	A	B	C	D	Maximum
NC					
12.6%N	0.4394	0.4394	0.4394	0.4394	0.4420
NGL	0.3207	0.3207	0.3207	0.3207	0.3183
EC	0.0180	0.0180	0.0180	0.0180	0.0177
RDX	0.1593	0.1488	0.1593	0.1496	0.1700
ATBC	0.0401	0.0455	0.0402	0.0452	0.0400
PbSalic	0.0052	0.0103	0.0148	0.0148	0.0050
CuSalic	0.0148	0.0148	0.0051	0.0098	0.0050
Graphite	0.0025	0.0025	0.0025	0.0025	0.0020
Predicted c^* [m/s]	1471.14	1458.05	1473.94	1460.25	1487.65
NASA CEA c^* [m/s]	1472.60	1458.50	1474.50	1460.70	1487.70
c^* relative deviation [%]	-0.1000	-0.03	-0.04	-0.03	-0.005
C_F	1.5769	1.5760	1.5763	1.5757	1.5770
I_{sp} [s]	236.70	234.31	236.92	234.61	239.15

The calculated specific impulse at sea level expansion for reference formulation, i.e. 225 s, seems coherent with the extruded double-base propellant range, while the I_{sp} numbers from Tab. 7 are in accordance with data for nitramine-added double-base propellants [3]. Thrust coefficients results will be applied in the next section.

RDX major role in enhancing theoretical c^* was evidenced from the contour plots so far presented, as well as from the Maximum c^* formulation in Tab. 7. Hence, taking Maximum c^* as a new reference blend for Cox response trace plotting, a possible path for further c^* enhancement may be devised. Fig. 4 depicts the resulting new Cox response trace plot. The same color coding as in Fig. 2 was adopted. Fig. 4 shows clearly the constant increasing c^* tendency stemming from augmenting RDX mass ratio, although this trend is limited by its upper limit defined in Tab. 1, i.e., 17 wt%. The effects of other components on c^* resemble the general trends discussed in Fig. 2. In short, there seems to exist room for further c^* improvement, following Cox's direction [45] for RDX. In effect, extrapolating the upper RDX mass ratio limit previously set, by adding up the mass ratio range of 10 wt.% to it, a new RDX upper mass ratio of 27 wt.% can be defined. If the remaining mass proportions of the compounds are kept constant, the resulting CMDB formulation, hereinafter labelled "Enhanced c^* ", allows a larger RDX mass content at the expense of the other propellant's components, according to Cox's direction approach [45]. This is shown in Fig. 5, which compares Maximum and Enhanced c^* CMDB formulations.

The Enhanced c^* formulation does not belong to the experimental region so far investigated and thus is not modelled by the fitted Scheffé polynomial depicted in Tab. 6. It yields a NASA CEA c^* of 1508.80 m/s, an I_{sp} of 242.54 s and a C_F of 1.5770. Regarding the reference double-base propellant described in Tab. 1, relative increments of 7.38 % and 7.80 % were attained for c^* and I_{sp} , respectively, by the Enhanced c^* formulation. The same observations made on Maximum c^* formulation, regarding its ballistic performance, are valid here. In short, the preliminary selection methodology herein discussed must be followed by an experimental characterization

program comprising, at least, production feasibility, compatibility assessment, chemical stability, mechanical properties, burn rate measurements in strand burner, and sensitivity responses under an appropriate testing program [60], while hazards management stems from proper selection of components [32], in order to thoroughly assess [3, 11] the candidate CMDDB formulations. Such characterization seems particularly important for Maximum and Enhanced c^* formulations, given some investigations regarding combustion stability, burning rates and mechanical responses [15, 54, 61, 62], as well as sensitivity reduction [28, 29] of nitrocellulose-based propellants as a function of RDX content and granulometry.

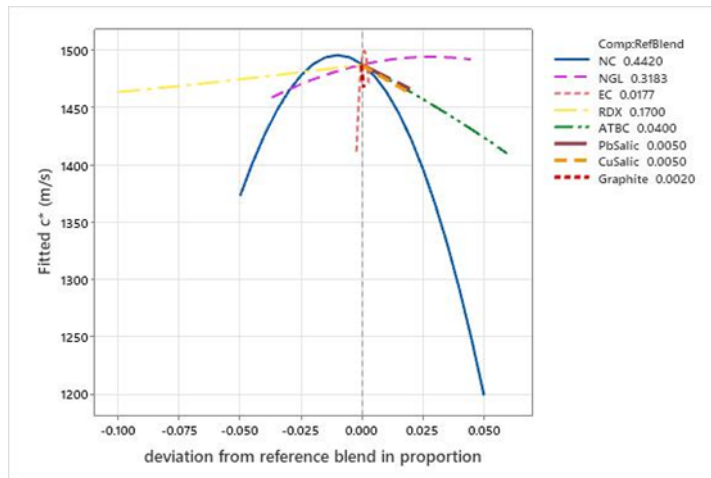


Fig. 4 Cox response trace plot for fitted c^* - Maximum c^* as the reference blend

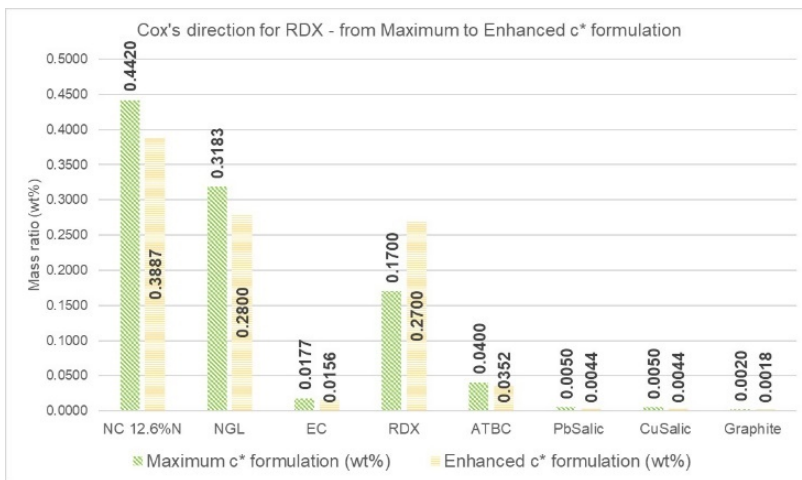


Fig. 5 Maximum and Enhanced c^* CMDDB formulations

Fig. 6 summarizes the theoretical c^* (left vertical axis) and sea-level expansion I_{sp} (right vertical axis) results for the six candidate CMDDB propellant formulations conceptually feasible, under a thermochemical perspective, to a 120 mm rocket assisted projectile. Reference formulation is also displayed, to illustrate the increase in

performance attained through the mixture modelling approach developed in this study. Enhanced c^* , Maximum c^* , A, B, C and D formulations are initial candidate possibilities in the CMDB family to be further experimentally investigated, for they yield better theoretical thermochemical performances, while conceptually offering lower vulnerabilities and greener profiles, as compared to the reference formulation.

In addition, a sequential design strategy [49] on theoretical c^* can be thought of, for instance, by adopting Enhanced c^* as a new centroid formulation and by redefining lower and upper mass ratios limits for the components [45]. Then again, Minitab® can generate a new experimental domain, following the steps previously detailed. Briefly, the fitting of theoretical characteristic velocity to a Scheffé-type model has shown itself useful for selecting promising formulations from a thermochemical standpoint and for opening a possible path for further improvement, perhaps circumventing costly and time-consuming trial-and-error experimental approaches.

Another advantage of the candidate formulations stems from their manufacture, without major changes in established production procedures [11]. They are expected to be produced under the standard solventless process, with RDX being included into the wet paste in the blending step, altogether with ATBC and the ballistic modifiers [3, 54].

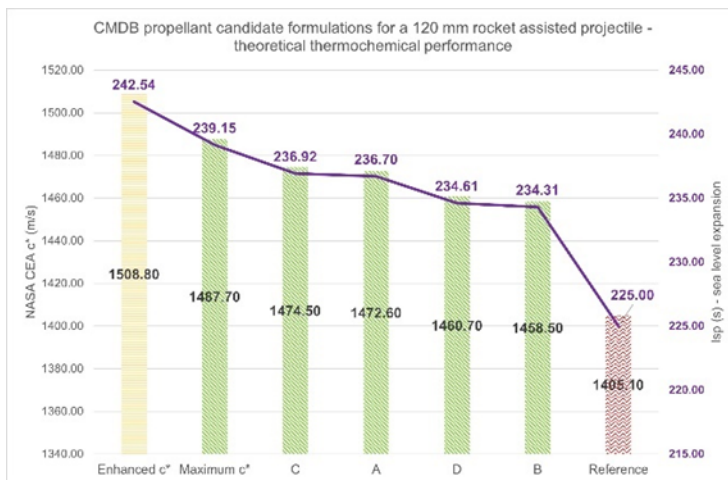


Fig. 6 Theoretical thermochemical performance of 120 mm RAP CMDB candidate formulations as compared to the reference formulation

3.2 Effect of Selected Propellant Formulations on the Design of a 120 mm Rocket Assisted Mortar Shell

Anti-personnel efficiency of rocket-assisted 120 mm grenade is 10 % lower than its counterpart filled solely by high explosive [12]. Hence, reducing the motor's volume within the shell without hampering its range extension seems a desirable trade-off approach between external and terminal ballistics. Szklarski et. al. [63] have undertaken a simultaneous assessment of range extension and accuracy improvement in a 155 mm artillery shell, showing that meeting both requirements can reduce the ratio of the explosive filling mass to the total mass of the projectile to as low as 15 % [63].

Under the rocket motor viewpoint, a valid question could be raised as to whether the volume of the propellant grain can be reduced, while keeping the intended range extension. Depending on its magnitude, this volume reduction would allow some alternatives to assure proper terminal effects, i.e., through a larger amount of explosive filling and/or by providing the round with steel fragments [63]. From the accuracy perspective, the volume reduction could lead to providing the shell with trajectory control devices [63]. The internal volume restrictions of 120 mm mortar shells make the trade-off among range extension, terminal effect, and accuracy even more daunting.

As a contribution to the subject, the six candidate CMDB formulations whose calculated thermochemical performances are displayed in Fig. 6 were investigated in terms of their resulting grain mass reductions, as compared to the reference formulation. To do so, it is necessary to calculate the mass of double-base propellant required to provide a maximum 50% range extension to a 120 mm mortar grenade, with a rocket motor operating under 850 N constant thrust [7], developed for 5 s [6, 7, 52]. The design constraints described by Kim et al. [7] are valid for these comparisons, i.e., a 16.40 kg 120 mm rifled shell, fired at a 45° angle, under a muzzle velocity of circa 380 m/s. As previously stated, Eq. (1) relates theoretical c^* to propellant's mass flow rate. From this equation, the required propellant's mass flow rate (\dot{m}) is calculated for a given set of values for thrust (F), thrust coefficient (C_F), and characteristic velocity (c^*). By defining the time interval (Δt) of the rocket motor operation under constant thrust, the required amount of propellant (m) to impart a 50% maximum range extension to a 120 mm mortar grenade, under 850 N constant thrust [7], is given by Eq. (2):

$$m = \frac{F}{C_F c^*} \Delta t \quad (2)$$

Fig. 7 depicts the results, both in absolute (left vertical axis) and relative (right vertical axis) terms. Color coding is the same as used so far. As expected, the trend is the opposite, to that outlined in Fig. 6. Among the selected candidate CMDB formulations, Enhanced c^* yielded the larger conceptual net mass reduction, i.e., nearly 0.130 kg, while keeping the maximum 50% range extension imparted to a 120 mm shell [7].

Assuming that the Enhanced c^* propellant achieves the necessary density and burn rate at the rocket motor's nominal chamber pressure [3], and that an appropriate grain geometry is used, the required average theoretical mass flow rate of 0.357 kg/s could be achieved. The resulting propellant's mass reduction could then diminish the volume occupied by the rocket motor. Subsequently, the newly available volume in the shell could bear a larger amount of explosive filling, thus favoring terminal effects. Conversely, the mass saving from the propellant could give way to some trajectory correction device, hence improving the projectile's accuracy. Interestingly, this approach, despite reducing the mass ratio between the solid propellant and the round, would not, in principle, hamper range extension [5, 9].

The initial calculations herein discussed, deriving from the candidate CMDB propellant formulations, suggest that improving thermochemical performance could effectively contribute to an acceptable trade-off among range extension, terminal ballistics, and accuracy in a 120 mm mortar RAP. A possible generalization of the developed method to other artillery projectiles, such as the 155 mm howitzer grenade, could be considered – provided that a suitable set of propellants is selected based on thermochemical calculations of c^* within an experimental region defined using the

mixture modeling technique. Next, given the thrust and time intervals of rocket motor operation necessary for a known range extension are available from literature data, specialized simulation codes or from actual field firings, theoretical c^* can be applied to preliminary estimations of the required amount of propellant in the rocket motor.

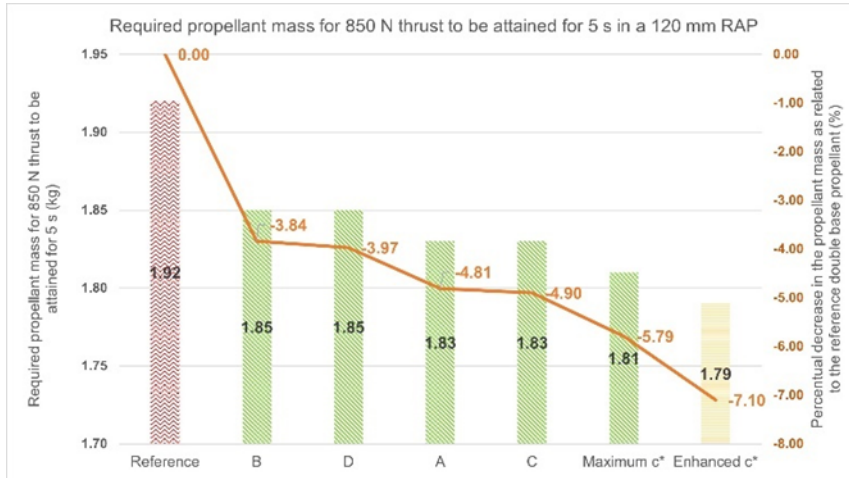


Fig. 7 Required propellant mass for 850 N thrust to be achieved for 5 s in a 120 mm RAP

4 Conclusions

The design of experiments-based methodology presented in this work has successfully led to the selection of six conceptually feasible double-base propellant formulations, under performance, low vulnerability, and human health/environmental constraints. The developed formulations simultaneously incorporate RDX, the inert plasticizer ATBC, as well as they reduce the total amount of the lead-based ballistic modifier, as compared to a literature-referenced composition.

The most promising propellant from this set resulted from a mixture modelling sequential path and allowed relative increments of 7.38 % and 7.80 % for theoretical c^* and I_{sp} , respectively, while yielding a conceptual net reduction in the propellant's mass of nearly 0.130 kg, regarding the reference double-base propellant. Bearing in mind that this reduction could be achieved while keeping the maximum 50 % range extension imparted to a 120 mm shell, there seems to exist room for efforts aiming at a trade-off among range extension, terminal effect, and accuracy even in a volume restricted system such as the 120 mm mortar projectile.

Effective application of the candidate CMDDB formulations, herein selected under a thermochemical viewpoint, to the assisted propulsion of a 120 mm mortar projectile is conditioned by the assessment of their industrial production feasibility, followed by the thorough examination of their chemical stability, compatibility, mechanical properties, burning rate, ballistic performance in static firings, and sensitivity responses. Getting a bigger picture is essential given the attempted conciliation among performance, low vulnerability, and environmental friendliness in the candidate CMDDB formulations. Finally, being part of a complex weapon system, the rocket motor must be integrated into the other elements of a 120 mm mortar round for field qualification.

The approach developed in this study is expected to turn preliminary selection of potentially feasible solid propellants formulations less arbitrary, thereby contributing to research efforts dedicated to the range extension of 120 mm mortar rocket-assisted artillery shells.

Acknowledgement

Portions of information contained in this publication are printed with permission of Minitab, LLC. All such material remains the exclusive property and copyright of Minitab, LLC. All rights reserved.

References

- [1] DAVENAS, A. The Main Families and Use of Solid Propellants. In: DAVENAS, A. (ed.). *Solid Rocket Propulsion Technology*. Oxford: Pergamon Press, 1993. pp. 329-367. ISBN 0-08-040999-7.
- [2] MANSON, M.P. *Guns, Mortars & Rockets*. 2nd ed. London: Brassey's Ltd, 1997. ISBN 1-85753-172-8.
- [3] SUTTON, G.P. and O. BIBLARZ. *Rocket Propulsion Elements*. 9th ed. Hoboken: Wiley, 2017. ISBN 978-1-1187-5388-0.
- [4] ARKHIPOV, V. and K. PERFILIEVA. Optimization of Construction of the Rocket-Assisted Projectile. In: *MATEC Web of Conferences*, 2017, **110**, pp. 8-13. DOI 10.1051/mateconf/201711001003.
- [5] SARHAN, A.M., M.A. EI-SENBAWI and A. NAFEA. Rocket Assisted Projectiles – A Computational Analysis of Trajectory. In: *International Conference on Aerospace Sciences and Aviation Technology*. Cairo: ASAT, 2003, **10**, pp. 267-277. DOI 10.21608/asat.2013.24426.
- [6] LIPANOV, A.M., S.A. KOROLEV and I.G. RUSYAK. Optimization of Aerodynamic Form of Projectile for Solving the Problem of Shooting Range Increasing. In: *AIP Conference Proceedings*. Novosibirsk: AIP, 2017, **1893**(1), 030085. DOI 10.1063/1.5007543.
- [7] KIM, K.-M., J.-H. CHO and D.-J. JEONG. Study on Composite Solid Propellants for Rocket Assisted Projectile. *Journal of the Korean Society for Aeronautical & Space Sciences*, 2010, **38**(11), pp. 1081-1086. DOI 10.5139/jksas.2010.38.11.1081.
- [8] UDDIN, M.N., H.K. BHUIYAN and G. MOSTOFA. An Experimental Investigation of Long-Range Projectiles under Different Wind Conditions. *American Journal of Mechanical Engineering*, 2021, **9**(1), pp. 7-17. DOI 10.12691/ajme-9-1-2.
- [9] FLEEMAN, E.L. Propulsion Considerations in Tactical Missile Design. In: SCHETZ, J. (ed.). *Tactical Missile Design*. Blacksburg: American Institute of Aeronautics and Astronautics, Inc., 2006. pp. 81-139. ISBN 978-1563477829.
- [10] *ARFSD-TR-99002 - 120-mm Ammunition Feasibility Assessment for Light Artillery* [Technical Report] [online]. 2000 [viewed 2024-11-22]. Available from: <https://apps.dtic.mil/sti/tr/pdf/ADA376461.pdf>
- [11] HERVÉ, A. Double-Base Propellants. In: DAVENAS, A. (ed.). *Solid Rocket Propulsion Technology*. Oxford: Pergamon Press, 1993. pp. 369-413. ISBN 0-08-040999-7.

- [12] MALBO, P. and C. BAR. New Insensitive Rifled 120-mm Mortar Ammunition with Enhanced Lethal Performance [online]. In: *Insensitive Munitions & Energetic Materials Technology Symposium*. Bristol: IMEMTS, 2006 [viewed 2024-11-25]. Available from: <https://imemg.org/eventsandmedia/imemts-bristol-2006/system/>
- [13] DAVENAS, A. *Solid Rocket Propulsion Technology*. Oxford: Pergamon Press, 1993. ISBN 0-08-040999-7.
- [14] KUBOTA, N. Combustion of Composite Propellants. In: KUBOTA, N. *Propellants and Explosives – Thermochemical Aspects of Combustion*. Weinheim: Wiley, 2002, pp. 157-197. ISBN 3-527-30210-7.
- [15] KUBOTA, N. Combustion of Double-Base Propellants. In: KUBOTA, N. *Propellants and Explosives – Thermochemical Aspects of Combustion*. Weinheim: Wiley, 2002, pp. 123-155. ISBN 3-527-30210-7.
- [16] KUBOTA, N. *Propellants and Explosives – Thermochemical Aspects of Combustion*. Weinheim: Wiley, 2002. ISBN 3-527-30210-7.
- [17] DEJEAIFVE, A., A. FANTIN, L. MONSEUR and R. DOBSON. Making Progress Towards «Green» Propellants. *Propellants, Explosives, Pyrotechnics*, 2018, **43**(8), pp. 831-837. DOI 10.1002/prop.201800026.
- [18] DEJEAIFVE, A., A. SARBACH, B. RODUIT, P. FOLLY and R. DOBSON. Making Progress Towards Green Propellants – Part II. *Propellants, Explosives, Pyrotechnics*, 2020, **45**(8), pp. 1185-1193. DOI 10.1002/prop.202000059.
- [19] POWELL, I.J. Insensitive Munitions – Design Principles and Technology Developments. *Propellants, Explosives, Pyrotechnics*, 2016, **41**(3), pp. 409-413. DOI 10.1002/prop.201500341.
- [20] *Munitions Safety Information Analysis Center (MSIAC)* [online]. [viewed 2024-07-09]. Available from: <https://www.msiac.nato.int/>
- [21] *Insensitive Munitions European Manufacturers Group (IMEMG)* [online]. [viewed 2024-07-09]. Available from: <https://imemg.org/>
- [22] SOTSKY, L., R. MAZZEI and N. AL-SHEHAB. Insensitive Munitions (IM) Enhancement of the 120 mm M934A1 High Explosive (HE) Mortar Cartridge. In: *Insensitive Munitions & Energetic Materials Technology Symposium*. Bristol, 2006.
- [23] HARA, M., W.A. TRZCIŃSKI, S. CUDZIŁO, M. SZALA, Z. CHYŁEK and Z. SURMA. Thermochemical Properties, Ballistic Parameters and Sensitivity of New RDX-Based Propellants. *Central European Journal of Energetic Materials*, 2020, **17**(2), pp. 223-238. DOI 10.22211/cejem/122326.
- [24] LIANG, T., Y. ZHANG, Z. MA, M. GUO, Z. XIAO, J. ZHANG, M. DONG, J. FAN, Z. GUO and C. LIU. Energy Characteristics and Mechanical Properties of Cyclotrimethylenetrinitramine (RDX)-Based Insensitive High-Energy Propellant. *Journal of Materials Research and Technology*, 2020, **9**(6), pp. 15313-15323. DOI 10.1016/j.jmrt.2020.09.132.
- [25] MEYER, R., J. KÖHLER and A. HOMBURG. *Explosives*. 7th ed. Weinheim: Wiley, 2015. ISBN 978-3-527-68959-0.
- [26] ELBASUNEY, S., A. FAHD, H.E. MOSTAFA, S.F. MOSTAFA and R. SADEK. Chemical Stability, Thermal Behavior, and Shelf-Life Assessment of Extruded

- Modified Double-Base Propellants. *Defence Technology*, 2018, **14**(1), pp. 70-76. DOI 10.1016/j.dt.2017.11.003.
- [27] ELBASUNEY, S., A.M.A. ELGHAFOR, M. RADWAN, A. FAHD, H. MOSTAFA, R. SADEK and A. MOTAZ. Novel Aspects for Thermal Stability Studies and Shelf-Life Assessment of Modified Double-Base Propellants. *Defence Technology*, 2019, **15**(3), pp. 300-305. DOI 10.1016/j.dt.2018.09.005.
- [28] YU, H., S. SUN, J. GAO, X. JIN, J. LIU and F. LI. Application of Nano-Sized RDX in CMDB Propellant with High Solid Content. *Propellants, Explosives, Pyrotechnics*, 2022, **47**(1). DOI 10.1002/prop.202100076.
- [29] LIU, J., X. KE, L. XIAO, G. HAO, Y. RONG, C. JIN, W. JIANG and F. LI. Application and Properties of Nano-Sized RDX in CMDB Propellant with Low Solid Content. *Propellants, Explosives, Pyrotechnics*, 2018, **43**(2), pp. 144-150. DOI 10.1002/prop.201700211.
- [30] BRINCK, T. Introduction to Green Energetic Materials. In: BRINCK, T. (ed.). *Green Energetic Materials*. Chichester: Wiley, 2014. ISBN 1-119-94129-6.
- [31] BÖHNLEIN-MAUB, J. and H. KRÖBER. The REACH Impact on Gun Propellant Formulations. *Propellants, Explosives, Pyrotechnics*, 2017, **42**(1), pp. 54-61. DOI 10.1002/prop.201600183.
- [32] *European Chemicals Agency* [online]. [viewed 2023-09-25]. Available from: <https://echa.europa.eu/>
- [33] *European Chemicals Agency – Search for Chemicals* [online]. [viewed 2024-05-26]. Available from: <https://echa.europa.eu/information-on-chemicals>
- [34] KUBOTA, N. *Propellants and Explosives – Thermochemical Aspects of Combustion*. Weinheim: Wiley, 2015. pp. 151-194. ISBN 3-527-69351-3.
- [35] WARREN, L.R., Z. WANG, C.R. PULHAM and C.A. MORRISON. A Review of the Catalytic Effects of Lead-Based Ballistic Modifiers on the Combustion Chemistry of Double Base Propellants. *Propellants, Explosives, Pyrotechnics*, 2021, **46**(1), pp. 13-25. DOI 10.1002/prop.202000167.
- [36] MARADEN, A., S. ZEMAN, J. ZIGMUND and M. MOKHTAR. Physical and Thermal Impact of Lead Free Ballistic Modifiers. *Thermochimica Acta*, 2018, **662**, pp. 16-22. DOI 10.1016/j.tca.2018.02.002.
- [37] JORGE, R.M. and A.A.M.F. FILHO. Characterization of New Lead-Free Ballistic Modifiers and Phthalate-Free Plasticizers in Propellants. *Journal of Aerospace Technology and Management*, 2019, **11**, pp. 15-18. DOI 10.5028/jatm.etmq.54.
- [38] GAŃCZYK-SPECJALSKA, K., K. CIEŚLAK, M. JAKUBCZAK, K. DROŹDŹEWSKA-SZYMAŃSKA, W.N. TOMASZEWSKI and P. PRASUŁA. The Effect of Citrate Plasticizers on the Properties of Nitrocellulose Granules. *Propellants, Explosives, Pyrotechnics*, 2023, **48**(6), e202200305. DOI 10.1002/prop.202200305.
- [39] *PubChem Compound Summary for CID 6505, Acetyl Tributyl Citrate* [online]. [viewed 2024-06-16]. Available from: <https://pubchem.ncbi.nlm.nih.gov/compound/Acetyl-tributyl-citrate>
- [40] FRYŠ, O., P. ČESLA, P. BAJEROVÁ, M. ADAM and K. VENTURA. Optimization of Focused Ultrasonic Extraction of Propellant Components Determined by

- Gas Chromatography/Mass Spectrometry. *Talanta*, 2012, **99**, pp. 316-322. DOI 10.1016/j.talanta.2012.05.058.
- [41] FURSTENAU, R. and R.W. HUMBLE. Thermochemistry. In: HUMBLE, R.W., G.N. HENRY and W.J. LARSON. *Space Propulsion Analysis and Design*. New York: McGraw-Hill Companies, Inc., 1995, pp. 149-178. ISBN 978-0-07-031320-0.
- [42] HUMBLE, R.W., G.N., HENRY and W.J. LARSON. *Space Propulsion Analysis and Design*. New York: McGraw-Hill Companies, Inc., 1995. ISBN 978-0-07-031320-0.
- [43] GORDON, S and B.J. McBRIDE. *Computer Program for Calculation of Complex Chemical Equilibrium Compositions and Applications - I - Analysis* [online]. 1994 [viewed 2024-06-18]. Available from: <https://ntrs.nasa.gov/api/citations/19950013764/downloads/19950013764.pdf>
- [44] GORDON, S and B.J. McBRIDE. *Computer Program for Calculation of Complex Chemical Equilibrium Compositions and Applications - II - User's Manual and Program Description* [online]. 1996 [viewed 2024-06-18]. Available from: <https://ntrs.nasa.gov/citations/19960044559>
- [45] CORNELL, J.A. *Experiments with Mixtures*. 2nd ed. New York: Wiley, 1990. ISBN 0-471-52221-X.
- [46] MONTGOMERY, D.C. Mixture Experiments. In: MONTGOMERY, D.C. *Design and Analysis of Experiments*. Hoboken: Wiley, 2020, pp. 461-472. ISBN 978-1-119-72210-6.
- [47] FREDERICK, R.A. and J.J. WHITEHEAD. Predicting Hybrid Propellant Regression Rate Using Response Surfaces. *Journal of Propulsion and Power*, 2009, **25**(3), pp. 815-818. DOI 10.2514/1.14418.
- [48] DE ARAÚJO, E.P., L.J. MASCHIO, L.G.F. PEREIRA, L.H. GOUVÊA and R. VIEIRA. Thermal, Viscosimetric and Thermomechanical Combined Assessment of Mixture Modelled Composite Fuels for Hybrid Propulsion. *Propellants, Explosives, Pyrotechnics*, 2022, **47**(4), e202100314. DOI 10.1002/prep.202100314.
- [49] BOX, G.E.P., J.S. HUNTER and W.G. HUNTER. *Statistics for Experimenters*. 2nd ed. Hoboken: Wiley, 2005. ISBN 0-471-71813-0.
- [50] MONTGOMERY, D.C. Experiments with Computer Models. In: MONTGOMERY, D.C. *Design and Analysis of Experiments*. Hoboken: Wiley, 2020, pp. 454-461. ISBN 978-1-119-72210-6.
- [51] BORGES, C.N., M.C. BREITKREITZ, R.E. BRUNS, L.M.C. SILVA and I.S. SCARMINIO. Unreplicated Split-Plot Mixture Designs and Statistical Models for Optimizing Mobile Chromatographic Phase and Extraction Solutions for Fingerprint Searches. *Chemometrics and Intelligent Laboratory Systems*, 2007, **89**(2), pp. 82-89. DOI 10.1016/j.chemolab.2007.06.002.
- [52] JEONG, J.-Y. and S.-H. CHOI. Propellant Characteristics Used for a Rocket-Assisted Projectile with Aluminium Contents. *Journal of the Korean Society for Propulsion Engineers*, 2019, **23**(5), pp. 60-66. DOI 10.6108/kspe.2019.23.5.060.
- [53] FAHD, A., H.E. MOSTAFA and S. ELBASUNEY. Certain Ballistic Performance and Thermal Properties Evaluation for Extruded Modified Double-Base Propellants. *Central European Journal of Energetic Materials*, 2017, **14**(3), pp. 621-635. DOI 10.22211/cejem/70206.

-
- [54] TUNESTÅL, E. Increased Impulse of Solventless Extruded Double Base Rocket Propellant by Addition of High Explosives RDX and FOX-7 [online]. In: *Insensitive Munitions & Energetic Materials Technology Symposium*. Portland: NDIA, 2018 [viewed 2024-09-18]. Available from: https://ndia.dtic.mil/wp-content/uploads/2018/imem/20152_Tunestal_Paper.pdf
- [55] *National Institute of Standards Chemistry Webbook* [online]. [viewed 2024-07-18]. Available from: <https://webbook.nist.gov/chemistry>
- [56] *NIST-JANAF Thermochemical Tables* [online]. [viewed 2024-07-18]. Available from: <https://janaf.nist.gov/>
- [57] PERRY, R.H. and D.W. GREEN (eds.). *Perry's Chemical Engineers' Handbook*. 8th ed. New York: McGraw-Hill, 2008. ISBN 0-07-154208-6.
- [58] SPEIGHT, J.G. (ed.). *Lange's Handbook of Chemistry*. 16th ed. New York: McGraw-Hill, 2005. ISBN 0-07-143220-5.
- [59] VATANI, A., M. MEHRPOOYA and F. GHARAGHEIZI. Prediction of Standard Enthalpy of Formation by a QSPR Model. *International Journal of Molecular Sciences*, 2007, **8**(5), pp. 407-432. DOI 10.3390/i8050407.
- [60] *MIL-STD-2105D*. Hazard Assessment Tests for Non-Nuclear Munitions [online]. 2011 [viewed 2024-09-18]. Available from: <https://imemg.org/wp-content/uploads/MIL-STD-2105D.pdf>
- [61] WANG, B.B., X. LIAO, L.T. DELUCA and W.D. HE. Effects of Particle Size and Content of RDX on Burning Stability of RDX-Based. *Defence Technology*, 2022, **18**(7), pp. 1247-1256. DOI 10.1016/j.dt.2021.05.009.
- [62] ZHANG, F., D.P. ZHU, Q. LIU, Z.T. LIU and P. DU. Study on the Effect of RDX Content on the Properties of Nitramine Propellant. *Defence Technology*, 2017, **13**(4), pp. 246-248. DOI 10.1016/j.dt.2017.05.020.
- [63] SZKLARSKI, A., R. GŁĘBOCKI and M. JACEWICZ. Impact Point Prediction Guidance Parametric Study for 155 mm Rocket Assisted Artillery Projectile with Lateral Thrusters. *Archive of Mechanical Engineering*, 2020, **67**(1), pp. 31-56. DOI 10.24425/ame.2020.131682.